Ground Verification of the Feasibility of Telepresent On-Orbit Servicing

Enrico Stoll and Ulrich Walter
Institute of Astronautics (LRT)
Technische Universität München
Garching 85748, Germany
e-mail: e.stoll@mytum.de, walter@tum.de

Jordi Artigas, Carsten Preusche, Philipp Kremer, and Gerd Hirzinger
Institute of Robotics and Mechatronics
German Aerospace Center (DLR)
Oberpfaffenhofen 82234, Germany
e-mail: jordi.artigas@dlr.de, carsten.preusche@dlr.de, philipp.kremer@dlr.de, gerd.hirzinger@dlr.de

Jürgen Letschnik
LSE Space Engineering & Operations AG
Wessling 82234, Germany
e-mail: juergen.letschnik@lsespace.com

Helena Pongrac
Human Factors Institute
University of the Bundeswehr
Neubiberg 85577, Germany
e-mail: helena.pongrac@unibw.de

Received 31 July 2008; accepted 6 January 2009

In an ideal case *telepresence* achieves a state in which a human operator can no longer differentiate between an interaction with a real environment and a technical mediated one. This state is called transparent telepresence. The applicability of telepresence to on-orbit servicing (OOS), i.e., an unmanned servicing operation in space, teleoperated from ground in real time, is verified in this paper. For this purpose, a communication test environment was set up on the ground, which involved the Institute of Astronautics (LRT) ground station in Garching, Germany, and the European Space Agency (ESA) ground station in Redu, Belgium. Both were connected via the geostationary ESA data relay satellite ARTEMIS. Utilizing the data relay satellite, a teleoperation was accomplished in which

Journal of Field Robotics 26(3), 287–307 (2009) © 2009 Wiley Periodicals, Inc.
Published online in Wiley InterScience (www.interscience.wiley.com). • DOI: 10.1002/rob.20286

the human operator as well as the (space) teleoperator was located on the ground. The feasibility of telepresent OOS was evaluated, using an OOS test bed at the Institute of Mechatronics and Robotics at the German Aerospace Center (DLR). The manipulation task was representative for OOS and supported real-time feedback from the haptic-visual workspace. The tests showed that complex manipulation tasks can be fulfilled by utilizing geostationary data relay satellites. For verifying the feasibility of telepresent OOS, different evaluation methods were used. The properties of the space link were measured and related to subjective perceptions of participants, who had to fulfill manipulation tasks. An evaluation of the transparency of the system, including the data relay satellite, was accomplished as well. © 2009 Wiley Periodicals, Inc.

1. INTRODUCTION

Spacecrafts are the only complex engineering systems without maintenance and repair infrastructure. Occasionally, there are space shuttle–based servicing missions, starting with the solar maximum repair mission (SMRM) in 1984, but there are no routine procedures foreseen for individual spacecrafts. Most malfunctioning spacecrafts require only a minor maintenance operation on orbit, a so-called on-orbit servicing (OOS) mission, to continue operational work. They have to be replaced due to the lack of OOS opportunities. The accomplishment of OOS missions would, similar to terrestrial servicing procedures, be of great benefit for spacecraft operators, because a wide spectrum of use cases exists as, e.g., spacecraft assembly, orbit transfer, maintenance and repair, resupply, or even safe deorbiting.

1.1. Motivations

Following the SMRM, there were several space transportation system (STS)–based servicing missions [e.g., Intelsat VI (F-3) and the Hubble Space Telescope (HST)]. These incipient OOS missions demanded not only a complex and cost-intensive shuttle mission but also the application of extravehicular activities (EVA). Astronauts had to leave the safe environment of the space station in order to retrieve and repair the spacecrafts in outer space, protected only by their suits.

Based on the criticality of an EVA, concepts of robotic applications have been developed that can be controlled by astronauts. However, devices such as the special-purpose dexterous manipulator (SPDM) by the Canadian Space Agency (Mukherji, Rey, Stieber, & Lymer, 2001) or the robotic astronaut (Robonaut) (Peters & Campbell, 1999), developed by the National Aeronautics and Space Administration (NASA), are in situ teleoperated by astronauts [from the space shuttle or the International Space Station (ISS)] and still demand the use of an STS.

In contrast to manned OOS missions, there are options to accomplish OOS missions unmanned. As will be seen in Section 1.2, unmanned spacecrafts (servicer satellites) are foreseen to accomplish OOS operations at a target satellite. For that purpose the explorative and manipulative possibilities of robots will be exploited to dock the servicer satellite with the malfunctioning target satellite and execute complex operations, remotely controlled from the ground.

Although much research has been undertaken on spacecraft autonomy, only a few space projects consider a telepresent control of the spacecraft, which is of special interest for the work presented here. A telepresent control includes a human operator in a ground station controlling the robotic application and receiving instantaneous (visual and haptic) feedback from the spacecraft to the actions. This work analyzes whether the concept of telepresence (control) is applicable to OOS. For that purpose a test environment that focuses on space applications in low Earth orbit (LEO) was developed and set up on the ground.

OOS in LEO is a special problem because direct contact between a ground station and the servicing spacecraft is given only in small time intervals. However, the feasibility of OOS operations is highly dependent on whether and how long a communication link between the controlling ground station and the servicer spacecraft can be established. Table I clarifies the reason. The space shuttle–based OOS missions of the HST are listed. Each of them required several EVAs resulting in a total EVA time of more than 24 h. An OOS mission that is telepresently controlled from the ground demands an equivalent amount of contact time.

Using direct communication in LEO would accordingly require several weeks or a complex ground station network. Because the HST orbits the Earth at

Table I. Space shuttle–based HST OOS missions.

Flight	Year	Number of EVAs	Total EVA time
STS-61	1993	5	35 h 28 min
STS-82	1997	5	33 h 11 min
STS-103	1999	3	24 h 33 min
STS-109	2002	5	35 h 55 min

approximately 570 km, there are four to eight orbit revolutions per day in which a human operator could steer a robotic servicer for a maximum 10 min per orbit revolution (Lundin & Stoll, 2006). Thus, for accomplishing complex OOS operations, the use of geostationary satellites is proposed, which increases the mean acquisition time of the spacecraft in LEO up to more than 1 h per orbit revolution. The use of geostationary data relay satellites, in turn, increases the round-trip delay of the signal, that is, the time between operator action and spacecraft feedback. The main goal of this work is to prove that the utilization of geostationary (GEO) data relay satellites for OOS is reconcilable with a telepresent control of the servicer spacecraft.

1.2. State-of-the-Art OOS Technology Demonstrators

This section gives a brief overview of OOS technology demonstrators that were brought to orbit, that are still orbiting Earth, or that are pending. The emphasis is hereby placed on the communication architecture (direct or relayed contact) and the manner of control (telepresence or autonomy).

The first robot in space that has been remotely controlled from ground was the Robot Technology Experiment (ROTEX) aboard the space shuttle Columbia in 1993. The operational modes were tele-sensor-programming (learning by showing), automatic (preprogrammed on the ground), and teleoperation onboard (an astronaut controlled the robot using a stereo monitor). Further, a teleoperation by a human operator from the ground, using predictive computer graphics, was performed (Hirzinger et al., 2004).

ETS VII is a Japanese engineering test satellite (ETS) capable of demonstrating bilateral teleoperation in space (Imaida, Yokokohji, Doi, Oda, & Yoshikawa, 2004). The spacecraft, consisting of a pair of satellites, was launched in 1997. Autonomous capturing of the smaller target satellite, inspection procedures, and a series of manipulation operations were demonstrated (Oda, 2000).

The robotic component verification aboard the ISS (Rokviss) is a German space technology experiment that was installed in 2005 outside the ISS at the Russian service module (Landzettel et al., 2006). Rokviss is a two joint robotic manipulator, controlled by a human operator via a direct radio link from the ground station in Weilheim, Germany (Preusche, Reintsema, Landzettel, & Hirzinger, 2006).

Experimental satellite system 10 (XSS-10) (Davis, 2005) was developed by the U.S. Air Force. The space mission was launched in 2003, and the mission objectives included autonomous navigation and proximity operations.

Experimental Satellite System 11 (XSS-11) (AFRL, 2007) was a microsatellite of approximately 100 kg. Launched in 2005, XSS-11 was designed for testing autonomous technologies necessary for the inspection of malfunctioning satellites.

All operations of the demonstration of autonomous rendezvous technology (DART) (Rumford, 2003) mission were developed to be autonomous. Launched to verify hardware and software for rendezvous and proximity operations, the main objectives were the demonstration of station keeping and collision avoidance maneuvers. However, when DART approached the target, it overshot an important waypoint and, thus, the preprogrammed transition to the target satellite, and collided with it. A premature retirement of DART was the consequence. The mission plan of Orbital Express (Boeing, 2007) foresaw the validation of software for autonomous mission planning, rendezvous, proximity operations, and docking. Further tests of robotic OOS scenarios included fuel and electronics transfer and deployment of and operations with a microsatellite. The Swedish Space Cooperation (SSC), together with Kayser-Threde, Germany, and Sener, Spain, is developing the SMART orbital life extension vehicle (SMART-OLEV) (Tarabini et al., 2007). It aims at extending the operational lifetime of geostationary satellites.

The Deutsche orbitale servicing mission (DEOS) (Sommer, 2003) will demonstrate diverse OOS scenarios such as rendezvous, inspection, formation flight, capture, stabilization, and controlled deorbiting of the target and servicer compound. In this connection two modes for commanding the servicer are foreseen. On the one hand, there will be active

ground control via telepresence, i.e., a control with instantaneous feedback to the human operator. On the other hand, it will also be possible to passively monitor autonomous operations from the ground. The ranger robotics program started in 1992 as the Ranger (Parrish & Akin, 1996) telerobotic flight experiment (RTFX) at the University of Maryland. The goal was to develop a dexterous extravehicular space telerobot with four robot manipulators and a free-flight capability in space. In 1996 the program got redirected as a shuttle launch payload to the ranger telerobotic shuttle experiment (RTSX), was financed until 2001, and never advanced from an engineering model.

The spacecraft for the universal modifications of orbits (SUMO) (Bosse et al., 2004) is a project by the Naval Research Laboratory and funded by DARPA. The main goal is to develop a spacecraft capable of demonstrating future OOS technologies. A series of autonomous rendezvous, grapple, and servicing experiments are planned.

Figure 1 shows a possible classification of the OOS demonstrators. The classification is based on two criteria. First, the options for *communication* with the OOS demonstrator (direct or relay to LEO or direct to GEO) in the respective orbit are considered. Second, the *round-trip delay* between operator command and received feedback is considered. Because a telepresent operation demands an instantaneous feedback to the operator's action, different natures of round-trip delay are defined. They are a first indication for the telepresence capability of the system.

The ideal or transparent telepresence (TTP) is, encouraged by the Rokviss experiments, here defined as being in the magnitude of approximately up to 0.1 s. This allows the user to obtain instantaneous feedback of the telecommands, and technical means will enable the human operator to feel present in the removed environment. It is followed by telepresence (TP), being in the magnitude of approximately up to 1.0 s. This is of special interest when considering applications that are either located in GEO or of which the communication has to be relayed via the GEO. The large physical distance, which the communication signal has to bypass in both cases, causes a minimum round-trip time

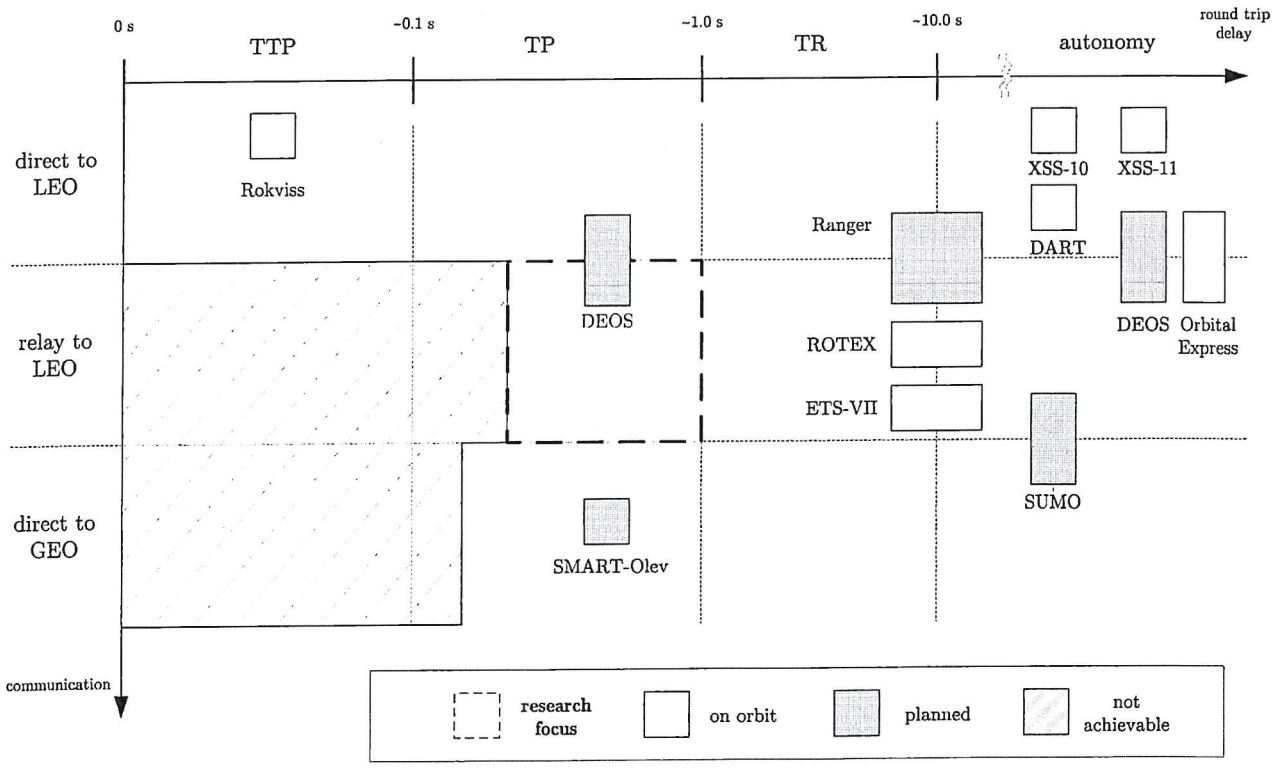

Figure 1. A classification of OOS demonstrators.

greater than 0.24 and 0.48 s, respectively. Therefore, the round-trip delay can be found in the telepresence branch. Transparent telepresence cannot be achieved for GEO or relay to LEO applications, as emphasized in Figure 1.

The third branch of the round-trip delay criteria, covering round-trip delays of approximately up to the 10.0-s magnitude, is defined as telerobotics (TR). This definition, encouraged by the ROTEX experiment, specifies an operation in which the operator has to cope with comparable large time delays. While working in a virtual reality with a three-dimensional (3D) model of the real environment, the human operator receives instantaneous simulated (predicted) feedback to the actions while they are executed in space a few seconds later and synchronized with the virtual reality afterward. It is evident that this approach is not usable for applications in which the environment is not sufficiently known, i.e., for an application of which either the 3D model or its dynamics is not known in detail.

Autonomy and supervisory control schemes, opposing direct telepresence, are considered as a field where the round-trip delay is not of importance because the operator on the ground is not actively involved in the operations.

1.3. Work Overview

As Figure 1 shows, most OOS demonstrators that are already on orbit utilized either the concept of TR or autonomy. For the addressed reasons, both are not reconcilable with the concept of telepresence. The preconditions for TTP do not hold for relayed communication, which in turn is necessary for complex and time-demanding operations in LEO. This work considers the telepresence branch in connection with a relay approach, as labeled in Figure 1.

To the authors' knowledge, no telepresence control with haptic feedback was executed via a geostationary relay satellite before. Thus, the work presents field experiments on Earth that demonstrate a telepresent teleoperation to a servicer in LEO. For that purpose a test environment was implemented, which included the ground station of the Institute of Astronautics (LRT) at Technische Universität München, Germany, and the ground station of the European Space Agency (ESA) in Redu, Belgium. They were connected via the ESA geostationary relay satellite ARTEMIS to set up a realistic environment. The robotic teleoperation that was executed comprised an OOS test bed developed by the Institute of Robotics and Mechatronics at the German Aerospace Centre (DLR) in Oberpfaffenhofen.

Section 2 deals with the communication architecture of the test environment, including the geostationary relay satellite. Section 3 describes in detail the robotic OOS test bed. Section 4 depicts performance and results of the experiments and clarifies how telepresence or the degree of telepresence can be evaluated. Section 5 closes the treatment of the ground verification of telepresence for OOS with concluding remarks and considers future direction for continuing research.

2. THE COMMUNICATION ARCHITECTURE

For verifying the feasibility of telepresent OOS in LEO, i.e., a telepresent servicing with fast feedback and relayed communication, a representative test environment was set up on the ground. For this purpose the two ground stations in Germany and Belgium were connected via the GEO ESA relay satellite ARTEMIS.

2.1. The Geostationary Relay Satellite ARTEMIS

The advanced relay technology mission (ARTEMIS) (Moens, Absolonne, & Lezy, 2003) was chosen to be the primary connector between the human operator and teleoperator, both located on the ground. ARTEMIS is the first European relay mission. It aimed at demonstrating new telecommunication techniques for data relay and mobile services. Launched in 2001 and designed for 10 years, it is now situated at approximately 21.45°E and is able to provide service to Africa and Europe.

Besides an optical link terminal and an L-band payload and a Ku-band payload as depicted in Figure 2 (left), ARTEMIS features an S- and K-band data relay (SKDR) payload. The latter was the focus of this work because the already-existing LRT ground station utilized the S-band frequency range. Using the SKDR payload, ARTEMIS communicates with its supporting ESA ground station in Redu, Belgium. Thereby, the feeder links (forward/return) are in Ka-band and in K-band, respectively. The link definitions can be seen in Figure 2 (right).

In the forward direction ARTEMIS can provide only one interorbit link (IOL) at a time, i.e., either S-band or Ka-band communication is supported.

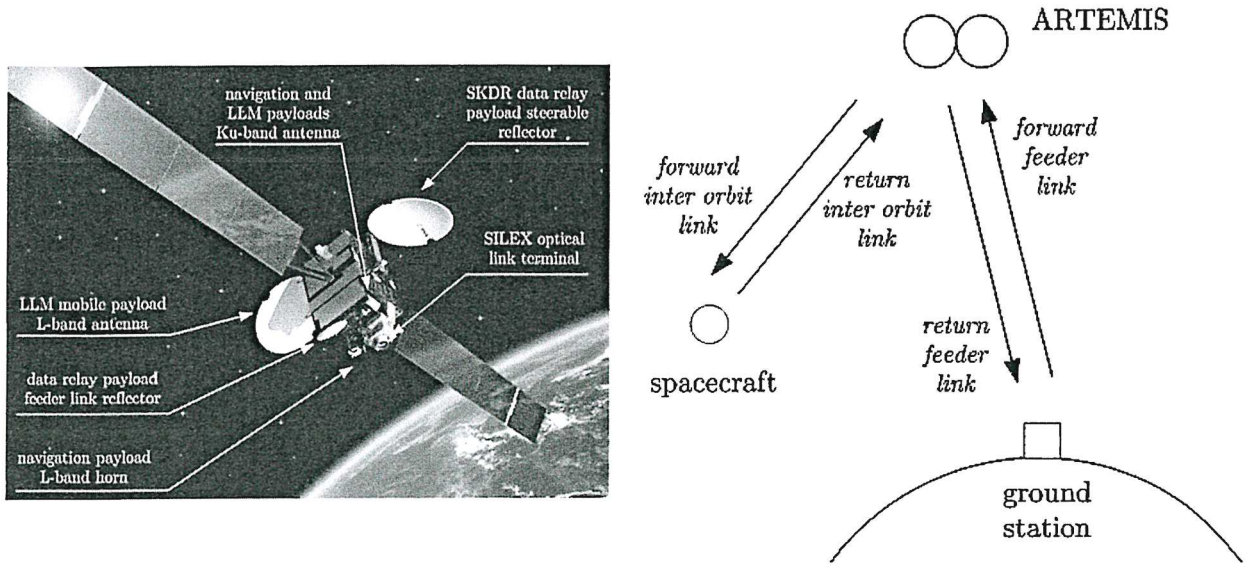

Figure 2. ARTEMIS and its antennas (Moens et al., 2003) (left) and ARTEMIS link definitions (right).

In contrast, in the return direction up to four IOLs can simultaneously be supported. Three of these channels can be allocated in the K-band, whereas the fourth channel supports the S-band frequency range. Accordingly, ARTEMIS cannot provide data relay between two communication end points using only the S-band. The feeder link (FL) works only in the K(a)-band. This fact is very important for the development of the communication architecture, which follows in the next section.

2.2. The Mirror Approach

The ARTEMIS transponder specifications given in the preceding section yielded a very specialized test setup of the telerobotic test environment (Stoll, 2008). The FL as well as the IOL of ARTEMIS had to be utilized because ARTEMIS cannot operate the IOL alone. The basic idea was to use both the ARTMEMIS FL and the IOL for communication to the ground. The Institute of Astronautics operates a ground station in the S-band frequency range, which is suitable for communicating via the IOL with ARTEMIS; that is, it represents the spacecraft (S/C) in orbit. Further, the ESA ground station in Redu and its K(a)-band equipment can be used to establish the FL, as depicted in Figure 3 (left). The human operator (HO) send telecommands (TC) via the data relay satellite (DRS) ARTEMIS to the teleoperator (TOP), situated in the LRT ground station (GS). After being executed, sensor data of the TOP are being transmitted as telemetry (TM) back to the OP.

This communication architecture is not suitable for fundamental telepresence experiments, as there is a large spatial distance between the human operator in Garching (near Munich), Germany, and the teleoperator in Redu, Belgium. This causes an increase in system complexity. Therefore, the existing experimental system was modified.

The selected communication architecture featured a so-called signal (radio frequency) mirror, as Figure 3 illustrates. All available radio links were used for transmitting TC data after they were generated by the HO located in Germany. That way it was possible to locate the TOP in Germany as well. That way the mirror was introduced in the Redu GS, which is basically a local bypass at the communication system (in particular the IMBU) (see Section 2.3). This means that the TC signal is reinjected immediately after reception into the uplink chain unchanged. Four hops[1] are used for the TC before the TOP receives and processes it. The control loop between the HO and TOP is closed locally (using TM data) with only one hop, which features a negligible time delay compared

[1]In computer or communication networks one hop is the path between two communication nodes, e.g., between routers on Earth or between a S/C and a GS, when considering space applications.

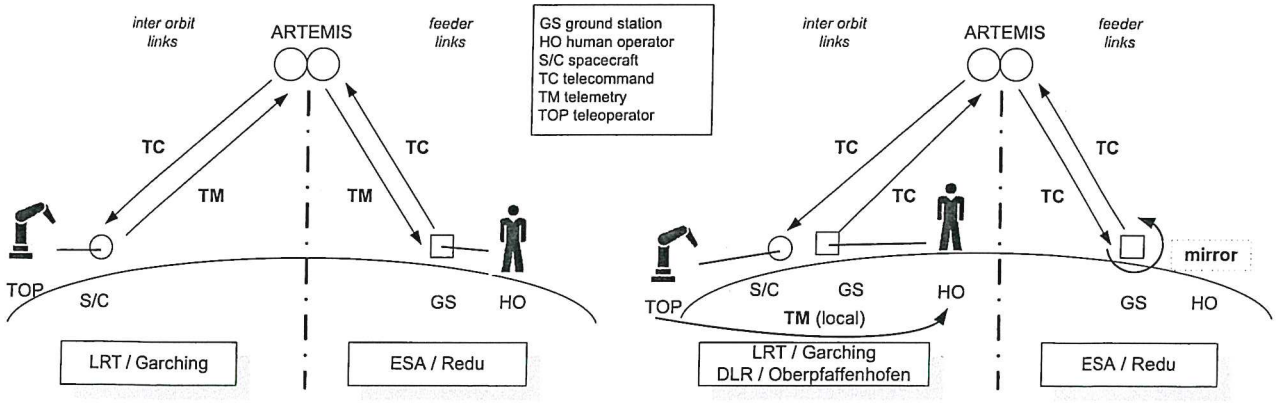

Figure 3. Communication architecture: (left) ideal and (right) using the mirror approach.

to the length of the TC hops. Thus, the round-trip delays that the operator perceives are identical for the ideal communication architecture and the mirror approach.

The advantage of this mirror approach is evident. The LRT ground segment can be used as the GS and the S/C of the experiment. Identical communication equipment can be used for both, because the same communication path (the IOL), with one frequency each for up- and downlink, is utilized. Further, no complex equipment that has to be remotely configured had to be installed at Redu.

2.3. The Communication Setup

As Figure 3 shows, the LRT ground segment has to feature all functionalities of a ground station, as well as of the spacecraft. This means that in forward and return directions, (almost) identical parameters (modulation, packet length, etc.) for configuring the communication link had to be used.

Traditional space missions show in contrast a very asymmetrical behavior considering downlink and uplink capacity. TM and TC data, usually being in the range of a few kilobits per second (kbps), are transmitted using a narrow band. Additionally, the data acquisition of a satellite payload (e.g., synthetic aperture radar applications for Earth observation) may necessitate the utilization of a broad band with the capability to download several megabits per second (Mbps). Table II shows typical maximum uplink/downlink data rates of space systems. Rokviss is an example that indeed shows the asymmetry but not to such a degree as, for example, Cryosat. The reason is that the robotic TC data have to be sent at a very high sampling rate.

For the mirror approach experiments presented here, this asymmetry had to be repealed. Uplink and downlink data rates are of the same because the data are identical. The haptic-visual feedback was realized locally, in order to not add delay.

Hence, an integrated modem and baseband unit (IMBU), as the core element of communications, was custom made by Satellite Services BV for the specific requirements of the test environment. Figure 4 shows a basic block diagram of the communication architecture. The DLR Institute of Robotics and Mechatronics, the LRT mission control center, and the LRT ground station are highlighted. Transmitting and receiving telepresence data at the LRT ground station was realized by utilizing the specialized radio frequency up- and downconverter in the S-band frequency range. The converters feature an adjustable oscillator, with which

Table II. Maximum data rates in uplink/downlink of exemplary space missions.

Satellite	Max. uplink/downlink
Terrasar-X	4 kbps/300 Mbps
Cryosat	2 kbps/100 Mbps
SMOS	4 kbps/18,4 Mbps
Rokviss	256 kbps/4 Mbps

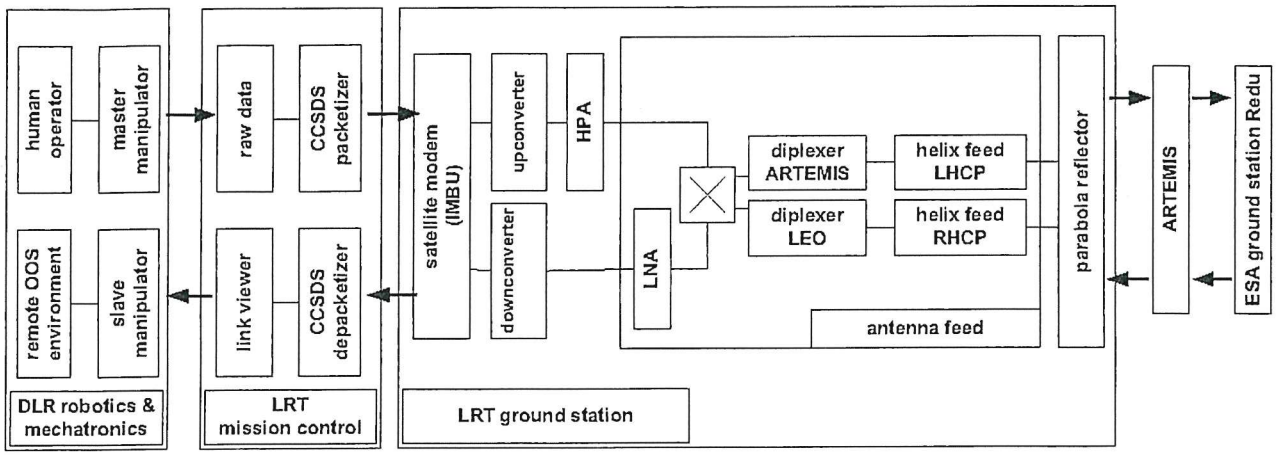

Figure 4. The communication setup of the telerobotic test environment.

the received or transmitted signal was mixed. This guaranteed a conversion between the intermediate frequency (70 MHz), which the IMBU utilized, and the frequencies of the receiver and the transmitter, respectively.

As seen in Figure 3 the ARTEMIS IOL forward and return links were used for S-band communication with the LRT ground station. Thus, frequencies had to be coordinated with the German federal network agency. The frequencies that have been allocated for the ARTEMIS service were 2,076.5 MHz for IOL return (ground station uplink) and 2,255.0 MHz for IOL forward (ground station downlink). Because these frequencies are usually used for communication in orbit, they were not usable on Earth without further regulations. Thus, the federal network agency allocated these frequencies only temporarily to LRT in the framework of an experimental radio communication license.

Broadband power amplifiers [high-power amplifier (HPA), low-noise amplifier (LNA)] had to be implemented into the test environment. The HPA was crucial for amplifying the upconverter signal to 20 W. This transmitting power results from the link budget and ensures that the requirements of an amplification of minimum +53.0 dB and a power output (at 1-dB compression point) of minimum +43.0 dBm were met. An according amplifier was not available off the shelf and was custom built by MITEQ.

Further, the antenna feed system (see Figure 4) had to be modified for the experiments because it had to support the communication with not only ARTEMIS in GEO but also conventional satellites in LEO. A flexible polarization switch was implemented into the setup. It allowed switching between the left-handed circular polarization (LHCP) of the IOL frequencies and the right-handed circular polarization (RHCP), which are used for ground-to-satellite communication. A gain-to-noise ratio $G/T > 4$ dB/K was realized by the setup and was sufficient for the telepresence experiments via the DRS.

ARTEMIS is a transparent satellite, i.e., received data are transmitted immediately after a frequency conversion. In contrast to so-called bent pipe technology, there is no demodulation, decoding, data correction, coding, and modulation done as for regenerative satellites. This makes the ARTEMIS less flexible than regenerative satellites but results in less processing time of data and accordingly supports the telepresence requirements of minimum round-trip delays.

3. THE BILATERAL CONTROL ARCHITECTURE OF THE OOS TEST BED

A test bed for telepresent OOS has been coupled to the LRT mission control center as illustrated in Figure 4. Located in the DLR institute of Robotics and Mechatronics in Oberpfaffenhofen, Germany, the test bed comprises two DLR lightweight robots (LWR) as a bilateral (force-coupled) master–slave system, and a target satellite dynamic emulator with an operations platform based on another LWR (Artigas, Kremer, Preusche, & Hirzinger, 2006).

As seen in Figure 5 a seven-degree-of-freedom (7DoF) LWR-III is used as haptic man–machine

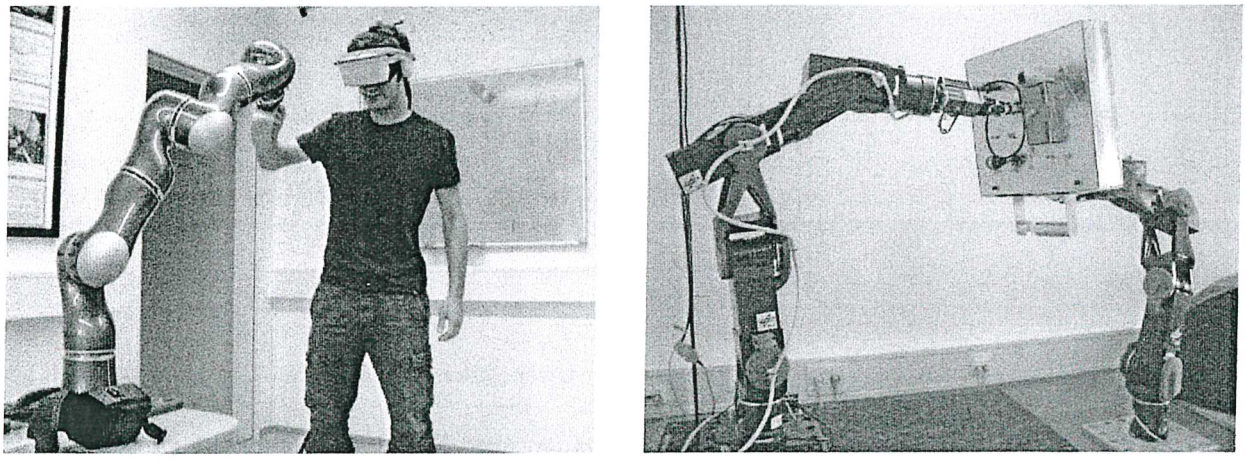

Figure 5. DLR OOS test bed.

interface. Further, a head-mounted display with stereo visualization is used to obtain an immersive implementation of the visual channel. A DLR LWR-II is used as a teleoperator robot that has been further equipped with an industrial gripper system in order to interact with the environment.

The OOS test bed has been designed to analyze different bilateral control strategies to cope with the presence of a different varying round-trip delays. The remote environment demonstrates a noncooperative, malfunctioning satellite emulated by means of another LWR-II with a satellite test board attached to the end effector of the robot. Featuring a deficiently working attitude control system, the satellite is tumbling in orbit and the operator has to fulfill two major tasks:

(a) Docking: The satellite platform is to be caught by means of the gripper. Once the task is achieved, the target satellite is considered to have no motion relative to the servicer satellite.
(b) Servicing: A series of servicing possibilities are given on the target satellite side, which the operator has to solve. The manipulation of a bayonet nut connector and a series of cables is foreseen.

The motion and force commands are measured and transmitted via the data relay satellite to the distant slave manipulator. This in turn tracks the commands of the master manipulator and feeds the interaction forces with the remote environment back to the master manipulator system. The human operator is thus energetically coupled to the remote environment through the electromechanical elements.

The inclusion of the human operator in the closed loop and the presence of the varying and comparably large time delay in the communication channel represents a challenging task.

Most approaches dealing with time-delayed haptic telepresence describe the system by means of power network elements, which are either designed to be passive (Anderson & Spong, 1989; Niemeyer, 1996) or will be adaptive in nature to keep passivity on the time domain (i.e., passivity not as a design constraint) (Artigas, Preusche, Hirzinger, Borghesan, & Melchiorri, 2008; Hannaford & Ryu, 2002).

One of the most remarkable approaches is the classical method of the scattering transformation or its wave variables formulation introduced in Anderson and Spong (1989) and Niemeyer (1996). By using the electrical-mechanical analogy, the wave variables transformation uses the power-conjugated variables of force and velocity to define wave variables the same way voltages and currents are related to energy waves in transmission lines. A *wavy* system has the interesting feature that passivity is preserved in the presence of a time delay. Thus, the two-port network created by a communication channel with time delay described in terms of wave variables is a passive system that will not alter stability for any amount of constant time delay.

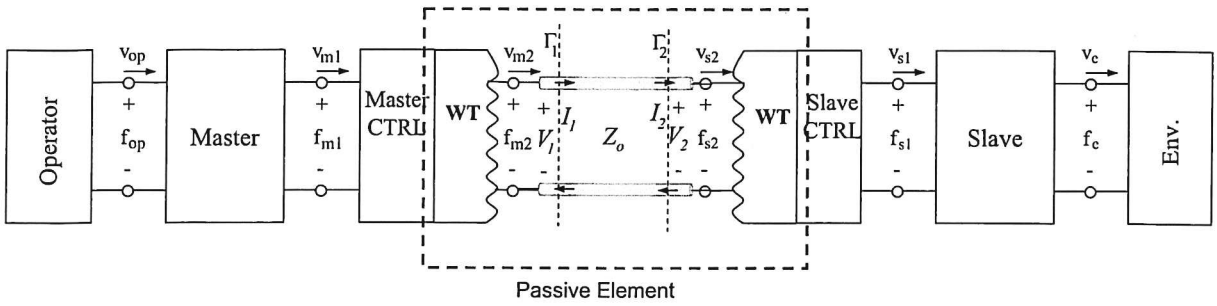

Figure 6. Wave-based position-force teleoperation control scheme.

The bilateral control method used here is based on the wave variables approach. The next subsections review the wave transformation and its passivity aspects and introduces a method to cope with the variation of the delay and the package loss.

3.1. Wave Variables with Constant Time Delay

Wave variables present an extension to the theory of passivity and are based on the concepts of power and energy. The transformed variables u and v are an algebraic relation of the power-conjugated variables $\dot{x}$ and F, velocity and force, respectively. u is the wave variable traveling from master to slave. v is the returning wave, from slave to master.

Figure 6 shows a wave variables–based position-force scheme. Two proportional–integral (PI) controllers at master and slave sites are responsible for minimizing the end effector position errors between master and slave, hence generating the required manipulation force on the slave site and haptic interaction forces on the master site. Note that the channel is *isolated* from the rest of the system by means of the wave transformers on each side of the channel, which in turn separates the power variables domain from the wave domain. The wave transformation equations for this scheme are Eq. (1) for the master site and Eq. (2) for the slave site, denoted by m and s, respectively. Here u represents the wave sent from the master to the slave and v the returning wave from the slave to the master:

$$u_m(t) = \frac{b\dot{x}_{md}(t) + F_m(t)}{\sqrt{2b}}, \quad v_m(t) = \frac{b\dot{x}_{md} - F_m}{\sqrt{2b}}, \tag{1}$$

$$u_s(t) = \frac{b\dot{x}_{sd}(t) + F_s(t)}{\sqrt{2b}}, \quad v_s(t) = \frac{b\dot{x}_{sd}(t) - F_s(t)}{\sqrt{2b}}. \tag{2}$$

Here b is the wave impedance constant, F_m and F_s are local controller force commands, and $\dot{x}_{md}$ and $\dot{x}_{sd}$ are desired motion velocities of the master and slave, respectively.

For the complete wave formulation please refer to Niemeyer (1996).

3.2. Passivity Condition with Varying Time Delay and Package Loss

Defining P_{in}, the power entering a system, as the scalar product between input vector x and output vector y and E_{store} as the stored energy of the system, the system is passive if and only if

$$\int_0^t P_{\text{in}} d\tau = \int_0^t x^T y d\tau \geq E_{\text{store}}(t) - E_{\text{store}}(0). \tag{3}$$

Without loss of generality, it can be assumed that the initial stored energy in the channel is equal to zero, $E_{\text{store}}(0) = 0$. Further, the forward and backward delays are assumed to be constant as a first estimation. Then the shift of wave signal can be formulated as follows:

$$u_m(t - T_{\text{fwd}}) = u_s(t), \quad v_m(t) = v_s(t - T_{\text{bwd}}). \tag{4}$$

In the wave domain, condition (3) leads to

$$\frac{1}{2}\left[\int_{t-T_{\text{fwd}}}^{t} u_m^2(\tau)d\tau + \int_{t-T_{\text{bwd}}}^{t} v_s^2(\tau)d\tau\right] \geq 0, \tag{5}$$

which holds true as long Eq. (4) (constant time delay and guarantee of signal delivery) does. Accordingly, the stability of the teleoperated system is guaranteed.

As seen in Section 2 the radio link from Garching–ARTEMIS–Redu imposes a set of

characteristics that produce a direct impact upon the bilateral control. The preceding section assumed an ideal delayed communication, with a constant time delay and zero package loss and bit error rates. In real scenarios, however, the delay cannot be considered constant and considerable package loss and bit error rates will be present.

The user datagram protocol (UDP) is used for network connection of LRT and DLR due to its fast exchange rate (the smaller the delay, the better the operation performance and transparency), but this protocol is subject to packet drops and reordering because the transmission is not controlled in the network layers.

Time-varying delay

Let forward and backward delays be defined by the time functions $T_{\text{fwd}}(t)$ and $T_{\text{bwd}}(t)$. Equation (4) can be reformulated:

$$u_m(t) = u_s[t + T_{\text{fwd}}(t)], \; v_m[t + T_{\text{bwd}}(t)] = v_s(t).$$

$T_{\text{fwd}}(t)$ and $T_{\text{bwd}}(t)$ functions are unknown at time t for the master and slave sent waves $u_m(t)$, $v_s(t)$, respectively. These functions can be identified only after transmission and delivery. Therefore the passivity condition in the form of Eq. (5) cannot be obtained. However, the passivity condition can be conserved by keeping the decoupled forward and backward channel lines passive, as follows:

$$E_{\text{comm,fwd}} = \frac{1}{2}\int_0^t \left[u_m^2(\tau) - u_s^2(\tau)\right]\mathrm{d}\tau \geq 0, \quad (6)$$

$$E_{\text{comm,bwd}} = \frac{1}{2}\int_0^t \left[v_s^2(\tau) - v_m^2(\tau)\right]\mathrm{d}\tau \geq 0. \quad (7)$$

Packet loss

Using the Internet as the communication medium will induce occasional packet drops and therefore information loss in the exchange line, in addition to jitter (variations of delay). The same is valid for satellite-based communication in which the time delay function is smoother and the data loss rate is lower. Both media are discrete time systems in which senders and receivers sample and pick the data with a certain frequency. An increase in time delay leads to the *empty sampling instances* for the receiver, which are usually called signal stretching in the continuous domain. The decrease in time delay leads to instances in which more than one data packet exists to be sampled at the receiver site. This is called signal compression in the continuous domain. However, only one signal can be sampled and the other will be discarded. This leads to information loss. It is important to notice that the wave information has energetic meanings. Another source of packet loss is the reordering of the sent signals, in which a later sent packet arrives earlier than an earlier sent packet. Typically empty sampling instances are solved by either inserting a zero value (null packet or zeroing strategy) or conveying the last valid signal, also known as hold-last-sample (HLS). It has been shown that none of them is sufficient for performance or stability conditions, and modifications should be applied to them (Hirche & Buss, 2004). The null packet strategy is lossy and overly conservative and leads to poor performance as well as wear and noise in mechanical parts. On the other hand, the HLS strategy keeps the transmitted wave form well but cannot guarantee the passivity of the channel and may lead to instability of the operation.

3.3. Proposed Method

For the sake of simplicity, the loss and time delay variations of the backward channel are neglected. Only the forward channel characteristics (dealing with backward link as ideal) are considered. After reformulating the continuous time expression in Eq. (6) for discrete time, the following relation is obtained:

$$2\Delta E(i)/T_s = \sum_{k=0}^{k=i} u_m^2(k) - \sum_{k=0}^{k=i} u_s^2(k), \quad (8)$$

where $\sum_{k=0}^{k=i} u_m^2(k)$ is the sum of the square of the right-moving wave variables and represents the power input to the forward communication block, $\sum_{k=0}^{k=i} u_s^2(k)$ is the sum of the received wave squares, which is the power output of the communication. T_s is the sampling time. The overall sent energy is calculated, and its value is sent through the time-delayed communication channel to the remote site (here slave). Hence, the remote receiver at time t receives knowledge on the overall energy sent up to a certain time instance (t^*). $t = nT_s$ is the current time, and $t^* = n^*T_s$ is the time stamp of the arrived packet. These two times are related by

$$nT_s = n^*T_s + T_{\text{fwd}}(n^*T_s). \quad (9)$$

To ensure passivity, it is sufficient to state

$$E_{\text{sent}}(n^*T_s) - E_{\text{received}}(nT_s) \geq 0. \tag{10}$$

Equation (10) is the *online forward observed energy* equation. The passivity of the channel has to be checked, comparing the overall energy input and output at the same time instances, but in practice the passivity condition cannot be measured online. Owing to the accumulative property of the sum of the sent wave energies, the following relation holds:

$$E_{\text{sent}}(n) \geq E_{\text{sent}}(n^*), \tag{11}$$

where $n > n^*$.

Considering the forward channel and renaming E_{sent} by E_m and E_{received} by E_s, and based on relation (11), the following relation is valid:

$$E_m(n) - E_s(n) \geq E_m(n^*) - E_s(n). \tag{12}$$

The left-hand side of relation (12) is the passivity condition, and the right-hand side is the online forward observed energy equation. Keeping the inequality in relation (10) leads to fulfilling the following overall passivity condition:

$$E_m(n) - E_s(n) \geq 0 \tag{13}$$

The online forward observed energy equation is used for online passivity checks. As is apparent, using this equation for passivity observation yields the system safety limits against the activity and the potential instability. A packet generator is implemented at each sender site, putting the algorithm's required information into a data structure. The information put into the sending packets are sending time stamp (n^*T_s), current sending wave value [$u_m(n^*)$], packet reception acknowledgment flag, summation of the overall sent wave [$T_s \sum_0^{n^*} u_m(n^*T_s)$], and the wave energy sent overall up to the current instance [$\frac{1}{2}T_s \sum_0^{n^*} u_m^2(n^*T_s)$]. The algorithm performs the following tasks to ensure the passivity. At each sampling time the packet reader on the receiver side checks the flag for arrival of data. When the flag indicates data arrival and their time stamp is bigger than the last recorded time stamp, the packet data will be processed. This process consists of one-step-ahead energetic checks and if the online energy observer violated the passivity condition, the current wave is modified to dissipate required energy and keep the passivity. The program checks the theoretical energetical impacts if the current wave was conveyed using Eq. (14). E_{curr} is the energy that the latest delivered wave could transmit to the system during one time sample:

$$E_{\text{curr}}(n) = \tfrac{1}{2}u_m^2(n^*)T_s. \tag{14}$$

The forward energy observer (E_{feo}) checks the safety of conveying the current arrived wave in Eq. (15). $E_{s_{\text{output}}}(n-1)$ is the energy output of the packet processor up to the current time, which is fed back to the algorithm, and $E_{\text{sent}}(n^*)$ is the sum of the energy sent from the master up to n^* instance:

$$E_{\text{feo}}(n) = E_{\text{sent}}(n^*) - E_{s_{\text{output}}}(n-1) - E_{\text{curr}}(n). \tag{15}$$

If Eq. (15) is bigger than or equal to zero, passivity would be kept by conveying $u_m(n^*)$. If Eq. (15) is negative, $u_m(n^*)$ has to be modified. In Eq. (17) the arrived $u_m(t^*)$ has to be changed in a way that dissipates the activity of $E_{\text{feo}}(n)$. If $\hat{u}_s^2(n) \geq 0$ is satisfied, a real answer exists and by using wave modification in one sample, the sensed activity can be dissipated. We can refer to $u_m(n^*)$ as $u_s(n)$. The modification is applied to $u_s(n)$, based on the following energy balance equation:

$$\tfrac{1}{2}u_s^2(n)T_s + E_{\text{feo}}(n) = \tfrac{1}{2}\hat{u}_s^2(n)T_s. \tag{16}$$

Based on this, $u_s(n)$ has to be modified to $\hat{u}_s(n)$ following

$$\hat{u}_s^2(n) = u_s^2(n) + \frac{2E_{\text{feo}}(n)}{T_s} \tag{17}$$

to dissipate the $E_{\text{feo}}(n)$ activity. The sign of the wave can be interpreted as a push or pull command. Even though wrong signature selection does theoretically not affect the energetic behavior of the channel, the correct solution is important. This is more significant when a blackout occurs in the line, and a high number of consequent losses are detected. The trend of the sent command (push or pull) is observable by comparing the currently arrived sum of the sent waves with the last valid recorded arrived sum in Eq. (18). n^{lvr} is the last-valid-recorded time instance of data

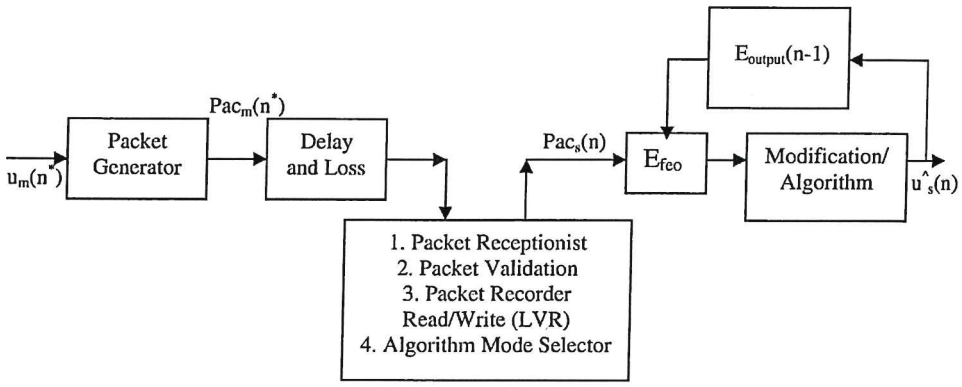

Figure 7. Scheme of the forward link packet processing and energy compensation.

arrival and is smaller than n^*:

$$S = \sum_{i=0}^{i=n^*} u_m(i) - \sum_{i=0}^{i=n^{lvr}} u_m(i). \tag{18}$$

When S is positive or negative, the trend indicates more push commands and more pull commands, respectively. Thus, the conveyed signal after a blackout can be calculated:

$$\hat{u}_s(n) = \frac{S}{|S|}\sqrt{u_s^2(n) + \frac{2E_{feo}(n)}{T_s}}. \tag{19}$$

For simple empty instances (due to reordering, occasional losses, or stretching) selection of the signature simply based on the current wave is correct but equation (19) generalizes these conditions as well.

If $\hat{u}_s^2(n) < 0$ holds, the wave is replaced with a zero, which is the maximum energy that can be dissipated in one instance. The remained undissipated energy is recorded to be dissipated in the next samples *if necessary*. As the activity detection in the forward observed energy equation is conservative and preemptive and is based on the worst possible case (sending zero command from counterpart), correction of this undissipated excess energy (remaining after zeroing) might not be necessary in the next steps. However, it is decided by the algorithm based on the received new data from the sender.

When the time stamp of the arrived packet is older than the last valid recorded time, the packet is discarded. (The algorithm has already dealt with this packet's absence energetically as another later-stamped-earlier-arrived packet. The receiver has information about the energy sent in between.) There can also be instances that simply no packets are delivered. In both cases the algorithm has to handle the empty instance. The algorithm assumes that the current wave should be equal to the last valid signal (HLS strategy). With this assumption the HLS signal should be checked in the previous algorithm for energy considerations. If necessary the same modifications introduced before will be applied on the waves. The scheme of the proposed method and the integration into the forward link are depicted in Figure 7.

4. PERFORMANCE AND RESULTS OF THE EXPERIMENTS

An objective evaluation of telepresence is difficult because the feeling of being immersed into the remote environment is dependent on the subjective perception of the individual. The immersion of the user is influenced by the modality of the feedback from the teleoperator. The modality in turn depends on the properties of the link that is used to transmit the feedback. Usually quality of service (QoS) criteria are used for evaluating terrestrial networks. Based on that, it has been shown (Chen, 2005; Park & Kenyon, 1999; Tfaily et al., 2003) that the QoS criteria *round-trip delay*, *jitter*, and *packet loss*, in the context of space communications often expressed in terms of *bit error rate*, can influence the task performance of a teleoperation.

The task performance of the human operator is directly related to the immersion of the human operator into the system and thus a measure for telepresence. Of the above criteria, the round-trip

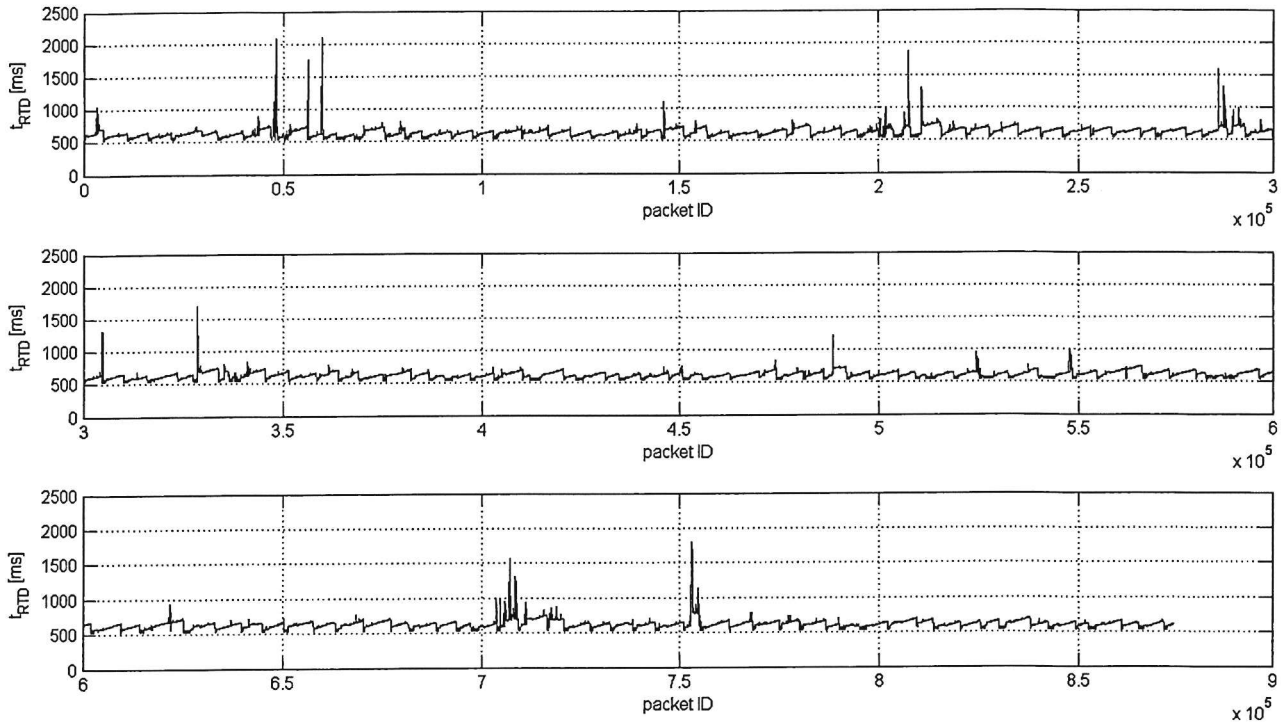

Figure 8. Round-trip delay characteristics of the telerobotic manipulation.

delay is the one considered as most critical for teleoperation because time delay can destabilize a telepresence system. Therefore, many approaches can be found in the literature to overcome the issues with network delays (Clarke-Griebsch, 2006; Hirche, Bauer, & Buss, 2005; Sheridan, 1993).

QoS criteria will initially be used for evaluating the telepresence capability of the system and related to the task performance of the human operator. For that purpose participants were asked to manipulate the OOS test bed under psychological instruction. The focus was laid on the task performance depending on the round-trip delay characteristics of the space link, i.e., the progression of the round-trip delay over time.

Finally, for a numerical determination of the telepresence capability of the system, an evaluation of the transparency of the system was undertaken.

4.1. Link Characteristics–Dependent Task Performance

Using the mirror approach, the signal from the master manipulator at DLR traveled to the LRT ground station, was transmitted to ARTEMIS, was forwarded to Redu, was mirrored, and was analogously redirected back to the DLR slave manipulator. According round-trip delay characteristics were generated. The characteristic involves the behavior of the round-trip delays over time. Round-trip delay characteristics with a mean round-trip delay of $\bar{t}_{RTD} = 622$ ms were obtained. Figure 8 shows a periodic behavior of the round-trip delay. Approximately every 1,000 packets the round-trip delay increases abruptly and decreases slowly afterward. This behavior is superimposed by fluctuations featuring a smaller span. Additionally, high peaks (>2,000 ms) occurred, which are caused by the comparable high amount of lost packets (≈5.8%). This in turn originates mostly from errors in the satellite modem, as a lot of received packets had incorrect checksums and to some minor degree from the use of UDP in the connection with the terrestrial WAN, because the space link itself featured <0.1% of lost packets. For evaluating the jitter of a signal, i.e., the variation in the round-trip delay, it has been reverted to the sample standard deviation s, because the samples can be considered as statistically (quasi) independent. The sample standard deviation

has been calculated to $s_t = 66$ ms, which means that approximately 68.3% of all data samples are located in the interval 622 ± 66 ms.

Bit error ratios (BERs) were measured within a dedicated BER test session. Usually the DRS service of ARTEMIS stops after 1 h for a couple of minutes. The reason is that the SKDR payload has to be recalibrated. Thus, BER tests were usually limited to approximately 1 h. However, ESA arranged an uninterrupted test session for 135 min, in which the BER could be measured. A BER of $<10^{-5}$ is regarded as standard acceptable for satellite telemetry and $<10^{-6}$ for the telecommand system. Thus the evaluated 8.3×10^{-8} can be considered as sufficient for satellite communication.

Large round-trip delays in the haptic and visual channel worsen task performance and telepresence feeling (Pongrac, 2008). This effect is in particular more distinct if the round-trip delays are varying. The tests, conducted within the framework of this work, second this fact. Using DRS for teleoperation increases the round-trip delay, which worsens the telepresence capability of a system in general. For an initial evaluation of the telepresence capability of the system, a group of participants was asked to take part in a psychological evaluation, consisting of *one exercise* and *two experimental trials*. Because of the limited availability of the ARTEMIS link, the group consisted of only six participants, who were completely unfamiliar with the system. Thus, the evaluation started with an exercise course. For becoming acquainted with the system, the bayonet nut connector (see Figure 5) had to be opened several times by means of the robotic manipulator under 0-s round-trip delay. The *exercise* was regarded as finished when the practice criterion was met, which was to fulfill the task within 30 s or in 25% of the time needed in the first trial. Afterward, the *experimental trials* started anew with 0-s round-trip delay. The remote environment, i.e., the noncooperative, malfunctioning satellite, started moving and the participants had to grip it via the slave manipulator. Once the handhold on the test board was caught, the requirements for a successful docking operation were considered as met. The time for performing the first task was measured. The satellite was brought to initial position, and no relative movement between the manipulator and satellite was further introduced. The opening anew of the bayonet nut connector was the second task to be fulfilled. This is quite a complex task for a teleoperation, because the participants had to grip the respective part of the connector and execute a turn to release it from the second part. For a final disconnection of both parts, the extraction had to be fulfilled exactly parallel to the board. Otherwise the parts cant and a disconnection is not possible. The performance time was again logged.

The second experimental trial was identical to the one executed earlier (0 ms), except for the round-trip delay. The two different tasks were performed using the ARTEMIS link and, thus, with a comparably high and not constant round-trip delay (see Figure 8). The participants had to answer three questions after the experimental trials:

- How natural did the interaction with the environment feel (*telepresence feeling*)? The scale ranged from 1 (very artificial) to 7 (very natural).
- How deeply did you feel immersed into the remote environment (*immersion into the system*)? The scale ranged from 1 (very weakly) to 7 (very deeply).
- In your opinion, of what magnitude was the round-trip delay?

The task performance of the group of participants that was measured is depicted in Figure 9. The figure shows that the task performance of the human operator decreases due to the use of the data relay satellite. Whereas the participants required (after a training phase) a mean of 15.0 s (with a sample standard deviation $\sigma = 13.1$ s) to grip the satellite

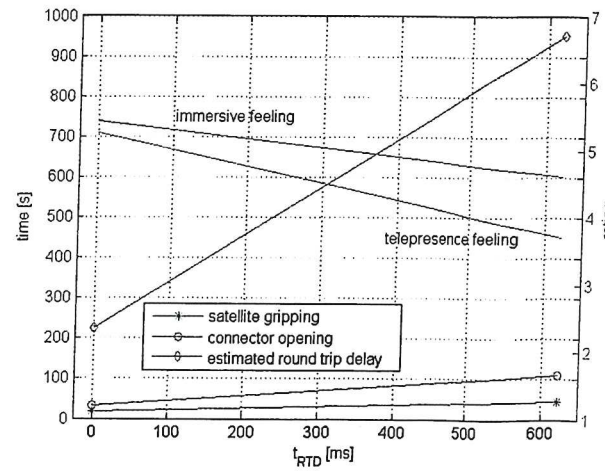

Figure 9. Mean task performance of participants.

without time delay, using the master manipulator, the gripping time increased to 44.8 s ($\sigma = 23.0$ s) in the presence of the DRS. The mean time for opening the bayonet nut connector more than tripled from 31.0 s ($\sigma = 15.1$ s) to 111.6 s ($\sigma = 94.7$ s). Further, the results show that the participants systematically overestimate the round-trip delay, even in the 0-ms case (estimated mean 226 ms). By using the ARTEMIS link the participants estimated the mean round-trip delay to be 952.6 ms ($\sigma = 587.0$ ms). The mean telepresence feeling (rating 1) dropped by 1.75 from 5.46 ($\sigma = 1.38$) to 3.71 ($\sigma = 1.35$), which corresponds from the psychological point of view to a rating decrement of 214%. The mean immersion into the system (rating 2) dropped by 0.55 points from 5.17 ($\sigma = 1.52$ s) to 4.62 ($\sigma = 1.47$ s), which corresponds to a rating decrement of 130%. Additional tests showed that there was no significant correlation between the demographical data of the participants (age, gender, handedness, etc.) and the experimental data. Therefore, the logged values were most likely dependent only on the experimental setup. Even though the number of participants was small, the tests clearly showed that all participants were able to fulfill the assigned tasks via the relay satellite in the presence of a round-trip delay. This will be the basis for additional tests.

4.2. Transparency Evaluation

A haptic man–machine interface (MMI) can be approximated as a device that generates mechanical impedance (Colgate & Brown, 1994). It represents the dynamic relationship between displacement (or velocity) and force. An ideal haptic interface would be capable of generating any impedance that is required to represent the remote environment realistically to the human operator. Accordingly, transparency can be considered as the accuracy in rendering the remote environment to the human operator (Hashtrudi-Zaad & Salcudean, 2001).

After stability, the major goal of any haptic telepresence system is transparency. Previous works (Lawrence, 1993; Yokokohji & Yoshikawa, 1994) exhaustively show that the pursuit of stability compromises transparency once the system constraints are established. In particular, the presence of delay in the communication channel leads to a conservative design of the control architecture, lowering the system transparency and, hence, the telepresence feeling in general. For a numerical confirmation of the above psychological evaluation of the teleoperation via ARTEMIS, a transparency evaluation of the master–slave system was conducted, which was based on the haptic feedback channel. This evaluation was conducted independently from the psychological evaluation and did not require any participants. For evaluating the performance of a teleoperated system, the *Z-width* concept was used.

4.3. The Z-Width Concept

The Z width is defined as the achievable range of impedance that the system can stably present to the operator (Colgate & Brown, 1994). Here the impedance to human $Z_{\text{toh}}(s)$ is defined by

$$Z_{\text{toh}}(s) = \frac{F_h(s)}{X_m(s)}. \tag{20}$$

The Z-width range is delimited by frequency-dependent lower and upper bounds. The lower bound of the Z width, $Z_{\min}(s)$, is calculated for $Z_e(s) \to 0$, and the upper bound, $Z_{\max}(s)$, is calculated for $Z_e(s) \to \infty$. That is,

$$\text{Free Motion: } Z_{\min}(s) = Z_{\text{toh}}(s)|_{Z_e(s)\to 0}. \tag{21}$$

$$\text{Constrained Motion: } Z_{\max}(s) = Z_{\text{toh}}(s)|_{Z_e(s)\to \infty}. \tag{22}$$

Consequently, the Z width is given by

$$Z_{\text{width}}(s) = Z_{\max}(s) - Z_{\min}(s). \tag{23}$$

This Z width allows comparison of different control schemes quantitatively. Because the bandwidth of human actuation and sensing capabilities is limited (Lawrence, Pao, White, & Xu, 2004), the analysis of the Z width in this paper will be restricted to the relevant frequency range.

4.4. Z-Width Measurement Procedure

If the human force and master position can be measured, then the human perceived impedance can be obtained from these measured signals using the least-squares input/output (LS I/O) identification method (Hirche, Stanczyk, & Buss, 2003). The goal of the identification method is to find the parameters of the transfer function of the human-perceived impedance that minimize the squared error between the real output and the output of the identified transfer function.

The following procedure is followed in order to measure the Z width out from the measured human percieved impedance:

1. measurement of the human operator force f_h and the master position x_m in the free movement case
2. I/O system identification of the transfer function $Z_{\text{toh}} = f_{h_{\text{free}}}/x_{m_{\text{free}}}$. This is the measured minimum limit of the Z width, $\hat{Z}_{\text{min}}$.
3. measurement of the human operator force f_h and the master position x_m in the case of wall contact
4. I/O system identification of the transfer function $Z_{\text{toh}} = f_{h_{\text{wall}}}/x_{m_{\text{wall}}}$. This is the measured maximum limit of the Z width, $\hat{Z}_{\text{max}}$.
5. The measured Z width, $\hat{Z}_{\text{width}}$, is the difference between the two identified impedances $\hat{Z}_{\text{width}} = \hat{Z}_{\text{max}} - \hat{Z}_{\text{min}}$.

Note that this evaluation was done only in one-dimensional space for obtaining scalar values for force and displacement. The two cases *free movement* and *wall contact* were generated by randomly moving the slave in free space and by moving the slave into a rigid wall (satellite), respectively. The progression of master displacement x_m and slave displacement x_s (in the time domain) is illustrated in Figure 10. The position of the slave (dashed line) follows the master (solid) after a round-trip delay, which is caused by the relay via the DRS. A wall is located at zero position. The free environment is indicated by a negative sign of the displacements. It can be seen that initially a movement in free environment has been conducted, followed by a movement into the virtual wall. The master displacement at that point in time becomes positive, whereas the slave motion is constrained by the wall. Thus, its displacement is almost constant at zero position.

Figure 11 shows the master and slave force in the time domain. The slave force is delayed by the DRS and features an opposite sign compared to the master force. Their absolute value is approximately identical in the free environment, and the absolute value of the slave force tends to be smaller. In contrast, for the wall condition the slave force increases to a multiple of the master force, considering absolute values. The values obtained this way were transferred into the frequency domain. Z_{min} and Z_{max} were derived and can be accessed from Figure 12. Because the impedances are complex values, they were plotted over the frequencies using a 20 log $|Z|$ scale to be compliant with a Bode representation. For approximating the transfer functions in Figure 12, appropriate time intervals for wall contact and free environment from Figures 10 and 11 were selected.

The corresponding Z_{width} is depicted in Figure 13. The Z-width concept is not an absolute indicator for system transparency. It can rather be utilized to evaluate the system transparency with respect to another system setup. For that reason the reference Z_{width} for 0 ms is also plotted in Figure 13. It can be seen

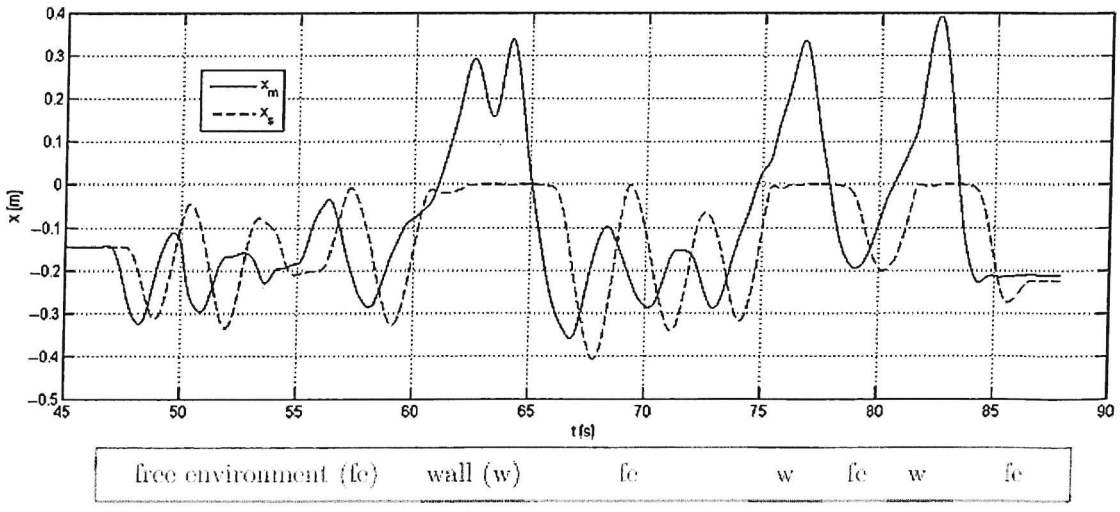

Figure 10. Displacement of master and slave over time.

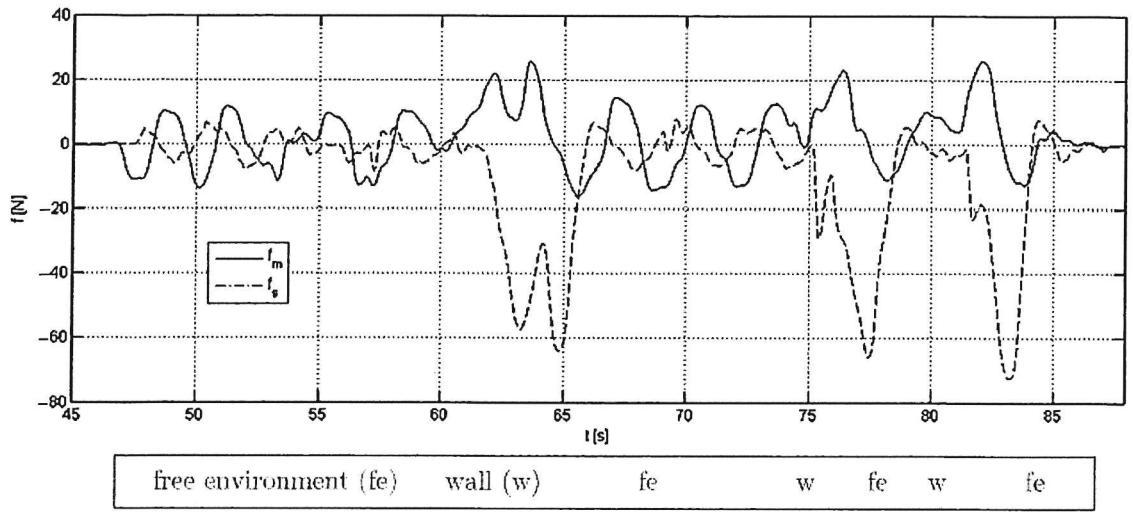

Figure 11. Force of master and slave over time.

that the increasing delay decreases the system transparency (in the low-frequency range), analogously to the task performance of the human operator. This is compliant with theory. In the low-frequency range the graphs can be assumed to be constant as a first approximation. It follows a peak (for the graphs with DRS), which is not of practical relevance because of the limits of the approximation.

The limits originate from the fact that the Z width is commonly derived by using a Padé series of finite order N to describe the time-delay system element D_t. By using a first-order series ($N = 1$),

$$D_t = e^{-sT} \approx \frac{1 - (T/s)}{1 + (T/s)}, \tag{24}$$

the Padé approximation is valid only for frequencies $\omega_{\text{lim}} < 1/(3T)$ (Hirche et al., 2005). Therefore, the peaks are of no practical relevance, because the Z-width graph is valid only for the low-frequency range.

The system frequency assigned to the abscissa can be interpreted as the frequency with which the

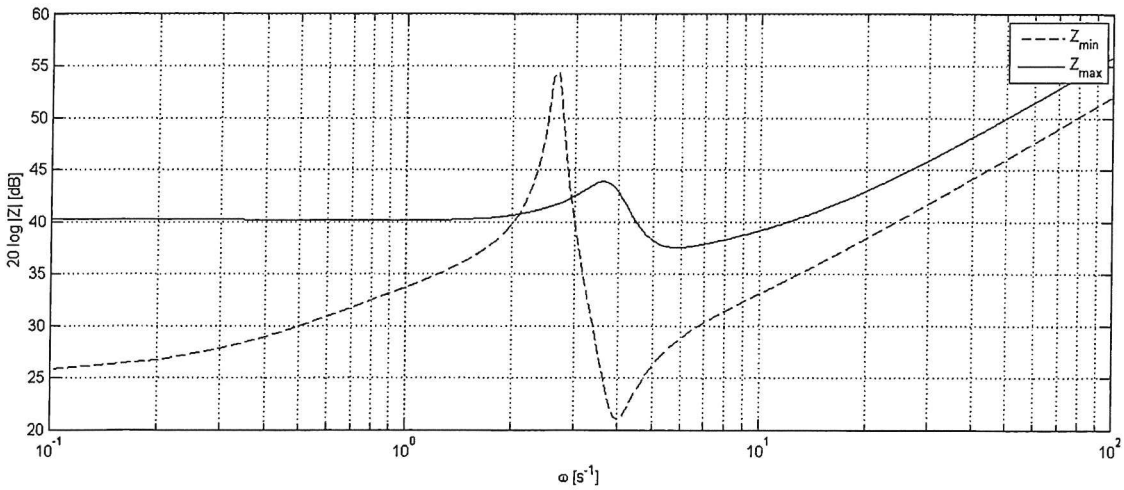

Figure 12. Absolute values for Z_{min} and Z_{max} via ARTEMIS.

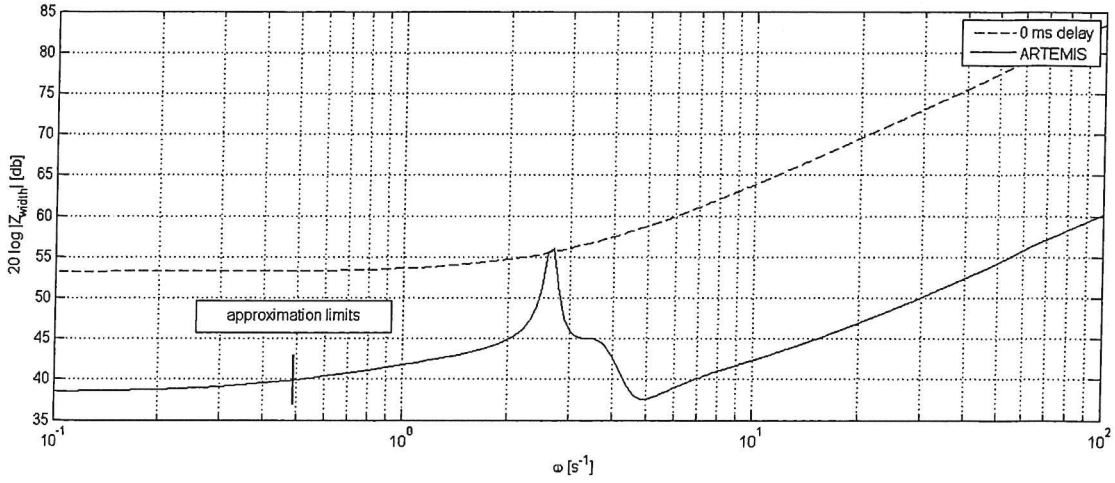

Figure 13. Absolute value of the Z width for zero delay and via ARTEMIS.

human operator steers the master manipulator. This is constrained by the limiting frequency and amounts in the given example to $\omega_{\text{lim}} \approx 0.5$ Hz. This limitation is of practical interest because it labels a region in which the system cannot react fast enough anymore, due to the occurring round-trip delay, to a given input. Accordingly, the user must not be allowed (by technical means as, e.g., inertia or damping) to execute teleoperations above this limiting frequency.

5. SUMMARY AND FUTURE DIRECTIONS

This work focused on utilizing the concept of telepresent control to OOS. In particular, the applicability to OOS missions in LEO, for which the communication has to be relayed via a DRS in geostationary orbit, was considered. This section summarizes the results and gives suggestions for future work.

5.1. Summary

The term telepresence describes a control concept in which a teleoperator is separated from the controlling human operator by a barrier. Telepresence demands that the human operator can hardly differentiate whether his impressions of feedback result from direct interaction with the environment or from technical means.

Utilizing telepresence for OOS operations promises a number of advantages for astronautics. On the one hand, the human operator is located on the ground and, thus, cost-intensive and critical EVAs can be avoided. On the other hand, it enables the human operator a real-time response to unforeseen incidents, which is not possible with autonomous OOS missions.

Contrary to terrestrial applications, the contact time to the teleoperator is limited, especially in LEO. Direct contact from the ground station to the servicing spacecraft is given for only a few minutes, which limits the data acquisition time. Hence, the use of geostationary satellites for data relay was considered, which increases the acquisition time by a multiple, compared to direct contact. However, the disadvantage of this approach is the increase in round-trip delay, jitter, and package loss.

It could be shown that by using the appropriate bilateral control strategy, this increase in round-trip delay and nonidealities does not conflict with the concept of telepresence control, for which a realistic feedback is demanded to some extent. A test environment was developed that was representative for telepresent OOS using a DRS and involved the Institute of Astronautics, the ESA, and the German Aerospace Center. A robotic OOS test bed was teleoperated via the ESA satellite ARTEMIS. The implementation of ARTEMIS and the setup on the ground enabled realistic measurements to be obtained, in order to evaluate the feasibility of telepresent OOS.

The obtained round-trip delays with a mean of 622 ms enabled accomplishment of the telepresent manipulation tasks, even under the influence of additional network delays.

For validating the above statement, a psychological evaluation was conducted. The feeling of telepresence or immersion into the system is a subjective perception. Thus, a number of participants were asked to steer the robotic scenario via ARTEMIS. The results show that it is possible to execute complex OOS maneuvers via a geostationary DRS and maintain the feeling of telepresence. This was corroborated by an evaluation of the system transparency. Based on that, the conclusion is drawn that telepresent OOS with haptic feedback via a geostationary relay satellite is feasible. Nonetheless, the number of participants was limited due to the availability of the satellite link. Thus, further testing will be needed to obtain a comprehensive human–machine evaluation.

5.2. Future Directions

Network delays are part of the considered round-trip delays. They can be minimized when realizing a telepresent space mission, by either locating the human operator in proximity to the ground station or by prioritizing the network link.

Future research has to consider the synchronization of system elements. The clock frequencies of signal-generating equipment and the communication equipment (e.g., IMBU) have to be adjusted with respect to each other in order to avoid peaks in round-trip delay. The necessity of system buffers and a sufficient buffer management will be of further interest. Optimizing the control parameters of the system holds even more potential for enhancing the system transparency than a minimized round-trip delay. The master–slave control architecture has to be adapted to the respective OOS operation to increase the telepresence capability.

By steering the robotic application via the DRS, the S-band link met its limits. The master sample rate had to be decreased to 500 Hz instead of the common 1,000 Hz. The stereo feedback (telemetry) had to be transmitted locally. Higher bandwidth is indispensable for space missions. The Ka-band frequency range is a possible alternative. This would also allow transmitting additional sensor data from the haptic-visual work space, which enhances the telepresence capability of the system. This in turn will support the immersion of the human operator into the system.

ACKNOWLEDGMENTS

This work is supported in part by the German Research Foundation (DFG) within the collaborative research center SFB453 "High-Fidelity Telepresence and Teleaction." The authors would like to express their sincere gratitude to the ESA ARTEMIS team for providing the opportunity to use the ARTEMIS relay satellite for telepresence experiments. In particular, we give special thanks to Benoit Demelenne and Damien Dessoy for prompt help and unbureaucratic scheduling concerning the data relay service. Further, we would like to thank LSE Space Engineering, DLR MORABA, Rhode & Schwarz, and DOMO TV for supporting the development of the LRT ground station.

REFERENCES

AFRL (2007). Xss-11 micro satellite—Fact sheet (Tech. Rep.). Kirtland Air Force Base, NM: Air Force Research Laboratory.

Anderson, R., & Spong, M. (1989). Bilateral control of teleoperators with time delay. IEEE Transactions on Automatic Control, 34(5), 494–501.

Artigas, J., Kremer, P., Preusche, C., & Hirzinger, G. (2006). Testbed for telepresent on-orbit satellite servicing. In Proceedings of the Human-Centered Robotics Systems Conference (HCRS), Munich, Germany.

Artigas, J., Preusche, C., Hirzinger, G., Borghesan, G., & Melchiorri, C. (2008, May). Bilateral energy transfer in delayed teleoperation on the time domain. In Proceedings of IEEE/RSJ International Conference on Robotics and Automation (ICRA'08), Pasadena, CA.

Boeing (2007). Orbital Express—Mission updates (Tech. Rep.). St. Louis, MO: Boeing.

Bosse, A. B., Barnds, W. J., Brown, M. A., Creamer, N. G., Feerst, A., Henshaw, C. G., Hope, A. S., Kelm, B. E., Klein, P. A., Pipitone, F., Plourde, B. E., & Whalen, B. P. (2004, August). Sumo: Spacecraft for the universal modification of orbits. Proceedings of SPIE, 5419, 36–46.

Chen, L. (2005, March). Effects of network characteristics on task performance in a desktop CVE system. In Proceedings of 19th IEEE International Conference on Advanced Information Networking and Applications, Tamkang, Taiwan (pp. 821–826).

Clarke-Griebsch, S. (2006). Overcoming network delays in telepresence systems with prediction and inertia. Ph.D. thesis, Lehrstuhl für Betriebswissenschaften und Montagetechnik, Technische Universität München, Munich, Germany.

Colgate, J., & Brown, J. (1994, May). Factors affecting the z-width of a haptic display. In IEEE International Conference on Robotics and Automation, San Diego, CA (vol. 4, pp. 3205–3210).

Davis, T. (2005, November). XSS-10 micro-satellite flight demonstration. In Proceedings of Georgia Institute of Technology Space Systems Engineering Conference, Atlanta, GA (GT-SSEC.D.3).

Hannaford, B., & Ryu, J.-H. (2002). Time domain passivity control of haptic interfaces. IEEE Transactions on Robotics and Automation, 18(1), 1–10.

Hashtrudi-Zaad, K., & Salcudean, S. E. (2001). Analysis of control architectures for teleoperation systems with impedance/admittance master and slave manipulators. International Journal of Robotics Research, 20(6), 419–445.

Hirche, S., Bauer, A., & Buss, M. (2005, August). Transparency of haptic telepresence systems with constant time delay. In Proceedings of IEEE Conference on Control Applications, Toronto, Canada (pp. 328–333).

Hirche, S., & Buss, M. (2004, December). Packet loss effect in passive telepresence systems. In 43rd IEEE Conference on Decision and Control (pp. 4010–4015).

Hirche, S., Stanczyk, B., & Buss, M. (2003, October). Transparent exploration of remote environments by internet telepresence. In Proceedings of the International Workshop on High-Fidelity Telepresence and Teleaction Jointly with the IEEE Conference HUMANOIDS, Munich, Germany.

Hirzinger, G., Landzettel, K., Brunner, B., Fischer, M., Preusche, C., Reintsema, D., Albu-Schäffer, A., Schreiber, G., & Steinmetz, M. (2004). DLR's robotics technologies for on-orbit servicing. Advanced Robotics—Special Issue Service Robots in Space, 18(2), 139–174.

Imaida, T., Yokokohji, Y., Doi, T., Oda, M., & Yoshikawa, T. (2004). Ground-space bilateral teleoperation of ETS-vii robot arm by direct bilateral coupling under 7-s time delay condition. IEEE Transactions on Robotics and Automation, 20(3), 499–511.

Landzettel, K., Preusche, C., Albu-Schäffer, A., Reintsema, D., Rebele, B., & Hirzinger, G. (2006, October). Robotic on-orbit servicing—DLR's experience and perspective. In Proceedings of the International Conference on Intelligent Robots and Systems (IROS), Beijing, China (pp. 4587–4594).

Lawrence, D. (1993). Stability and transparency in bilateral teleoperation. IEEE Transactions on Robotics and Automation, 9(5), 624–637.

Lawrence, D., Pao, L., White, A., & Xu, W. (2004, March). Low cost actuator and sensor for high-fidelity haptic interfaces. In Proceedings. 12th International Symposium on Haptic Interfaces for Virtual Environment and Teleoperator Systems, 2004. HAPTICS '04 (pp. 74–81).

Lundin, R., & Stoll, E. (2006, October). Coverage time variation in a near-earth data relay satellite system. In 57th International Astronautical Congress, Valencia, Spain.

Moens, C., Absolonne, F., & Lezy, C. (2003). Artemis data relay payload iot results as measured from Redu in Feb/Mar 2003 (Tech. Rep.). Redu, Belgium: European Space Agency.

Mukherji, R., Rey, D., Stieber, M., & Lymer, J. (2001, June). Special purpose dexterous manipulator (SPDM) advanced control features and development test results. In Proceedings of the 6th International Symposium on Artificial Intelligence and Robotics and Automation in Space (i-SAIRAS), St-Hubert, Canada.

Niemeyer, G. (1996). Using wave variables in time delayed force reflecting teleoperation. Ph.D. thesis, Department of Aeronautics and Astronautics Engineering, Massachusetts Institute of Technology, Cambridge, MA.

Oda, M. (2000, April). Experiences and lessons learned from the ETS-vii robot satellite. In IEEE International Conference on Robotics and Automation, 2000. Proceedings. ICRA '00, San Francisco, CA (vol. 1, pp. 914–919).

Park, K., & Kenyon, R. (1999, March). Effects of network characteristics on human performance in a collaborative environment. In Proceedings of IEEE International Conference on Virtual Reality, Houston, TX (pp. 104–111).

Parrish, J., & Akin, D. (1996, June). The ranger telerobotic flight experiment: Mission, technologies, and programmatics. In Proceedings of Conference on Robotics for Challenging Environments, Albuquerque, NM (pp. 136–142).

Peters, R., II, & Campbell, C. (1999, September). Robonaut task learning through teleoperation. In Proceedings of IEEE International Conference on Robotics and Automation, Taipei, Taiwan (pp. 2806–2811).

Pongrac, H. (2008). Gestaltung und Evaluation von virtuellen und Telepräsenzsystemen an Hand von Aufgabenleistung und Präsenzempfinden. Ph.D. thesis, Human Factors Institute, Universität der Bundeswehr, Neubiberg, Germany.

Preusche, C., Reintsema, D., Landzettel, K., & Hirzinger, G. (2006, October). ROKVISS—Preliminary results for telepresence. In Proceedings of the International Conference on Intelligent Robots and Systems (IROS), Beijing, China (pp. 4595–4601).

Rumford, T. (2003, April). Demonstration of autonomous rendezvous technology (DART) project summary. In Proceedings of Space Systems Technology and Operations Conference, Orlando, FL (pp. 10–19).

Sheridan, T. (1993, October). Space teleoperation through time delay: Review and prognosis. IEEE Transactions on Robotics and Automation, 9(5), 592–606.

Sommer, B. (2003, October). Automation and robotics in the German space program—Unmanned on-orbit servicing (OOS) and the TECSAS mission. In Proceedings of 55th International Astronautical Congress, Vancouver, Canada.

Stoll, E. (2008). Ground verification of telepresence for on-orbit servicing. Ph.D. thesis, Institute of Astronautics, Technische Universität München, Munich, Germany.

Tarabini, L., Gila, J., Gandiaa, F., Molinaa, M. A., Del Curab, J. M., & Ortegac, G. (2007, October). Ground guided CX-OLEV rendezvous with uncooperative geostationary satellite. Acta Astronautica; Selected Proceedings of the 57th IAF Congress, Valencia, Spain (vol. 61, pp. 1–6).

Tfaily, R., Gaiti, D., Pujolle, G., Wai, Y., Qiang, G., & Marshall, A. (2003, October). Haptic virtual environment performance over IP networks: A case study. In Proceedings of 7th IEEE International Symposium on Distributed Simulation and Real-Time Applications, Delft, The Netherlands (pp. 181–189).

Yokokohji, Y., & Yoshikawa, T. (1994). Bilateral control of master-slave manipulators for ideal kinesthetic coupling-formulation and experiment. IEEE Transactions on Robotics and Automation, 10, 605–620.

VOLUME 26 ISSUE 3 MARCH 2009

SPECIAL ISSUE ON SPACE ROBOTICS, PART I

Papers published online in Wiley InterScience. www.interscience.wiley.com/journal/rob.

JOURNAL OF FIELD ROBOTICS

WILEY Publishers Since 1807

ISSN 1556-4959

Editor:
SANJIV SINGH

Guest Editors:
TERRENCE FONG
KEIJI NAGATANI
DAVID WETTERGREEN